# 10

# Deep controls on intraplate basin inversion

SØREN B. NIELSEN, RANDELL STEPHENSON, AND CHRISTIAN SCHIFFER

**Abstract**

Basin inversion is an intermediate-scale manifestation of continental intraplate deformation, which produces earthquake activity in the interior of continents. The sedimentary basins of central Europe, inverted in the Late Cretaceous–Paleocene, represent a classic example of this phenomenon. It is known that inversion of these basins occurred in two phases: an initial one of transpressional shortening involving reverse activation of former normal faults and a subsequent one of uplift of the earlier developed inversion axis and a shift of sedimentary depocentres, and that this is a response to changes in the regional intraplate stress field. This European intraplate deformation is considered in the context of a new model of the present-day stress field of Europe (and the North Atlantic) caused by lithospheric potential energy variations. Stresses causing basin inversion of Europe must have been favourably orientated with respect to pre-existing structures in the lithosphere. Furthermore, stresses derived from lithospheric potential energy variations as well as those from plate boundary forces must be taken into account in order to explain intraplate seismicity and deformation such as basin inversion.

## 10.1 Introduction

The focus of this chapter is intraplate stress and deformation in the European continent and the adjacent North Atlantic area. By "deep controls" we understand the involvement of the whole crust and mantle lithosphere, i.e., the lithosphere-scale processes involved in intraplate deformations such as basin inversion, which includes dynamic interactions with the underlying mantle. We will not be concerned with the relationship between basement faulting and the related folding and faulting of the overlying sediments. An extensive literature covers this subject from an observational, experimental, and modelling point of

*Intraplate Earthquakes*, ed. Pradeep Talwani. Published by Cambridge University Press. 

view, and we refer to the review by Turner and Williams (2004) and the references quoted therein.

One of the fundamental problems of geoscience is to link cause and effect on a regional scale and many million years back in time. What are the causative events that result in intraplate deformation? The North Atlantic realm and the European continent furnish excellent present and past examples of the existence and action of intraplate stresses originating from different sources.

In the past, some 65+ Ma ago, the generally north–south convergence of Africa and Europe during the Late Cretaceous (e.g., Rosenbaum *et al.*, 2002) furnishes an example of stresses transmitted into the interior of the European plate causing compressional shortening of sedimentary basins and rifts in the Alpine foreland, and hence their inversion (Ziegler, 1987, 1990). These relatively mild intraplate continental deformations have in Europe become known as "basin inversion" and the locations of the main examples are sketched out in Figure 10.1. The term "basin inversion" describes the process when an elongate zone of a former area of subsidence – a sedimentary basin or a continental rift – reverses its vertical direction of movement and becomes uplifted and eroded (Ziegler, 1987). The concept was first considered on a regional scale in the European continent by Voigt (1962). With the work of Ziegler (1987, 1990) the concept was placed in a plate tectonic framework involving a causal relationship between stress-producing processes at plate boundaries (the Africa–Europe collision) and stress-induced deformation in the interior of the European continent.

At the present day, the North Atlantic depth Anomaly (NAA), related to the magmatic opening of the North Atlantic around 56 Ma (Tegner *et al.*, 1998) and still visible in the melt anomaly of Iceland and the anomalously shallow North Atlantic Ocean, is a source of excess lithospheric potential energy and anomalous mantle pressure, which causes stresses that propagate through the lithosphere into the surrounding continental plates.

In this chapter, keeping in mind our goal to link cause and effect, we start with an overview of the present-day stress field of the North Atlantic–European realm placed in the context of the NAA (Section 10.2), something reasonably well known, in order to make inferences about present-day lithosphere processes that "cause" intraplate stresses and, possibly, deformation. This is followed by an overview of past (~65 Ma) intraplate deformation in Europe and how it occurred (the "effect"), as expressed by the geological record and predictive models of "basin inversion" (Section 10.3), and a discussion on how this might inform us as regards the link between intraplate forces and strain in continents in general (Section 10.4).

## 10.2 Present-day intraplate stress in the Europe–North Atlantic area

A range of stress sources contribute to the stress state of the lithosphere. These include (e.g., Ranalli, 1995) slab pull, shear resistance at subduction zones and strike slip faults, convection drag at the base of the lithosphere, stresses transferred to the interior of plates from plate boundary processes, horizontal gradients of lithospheric potential energy, and

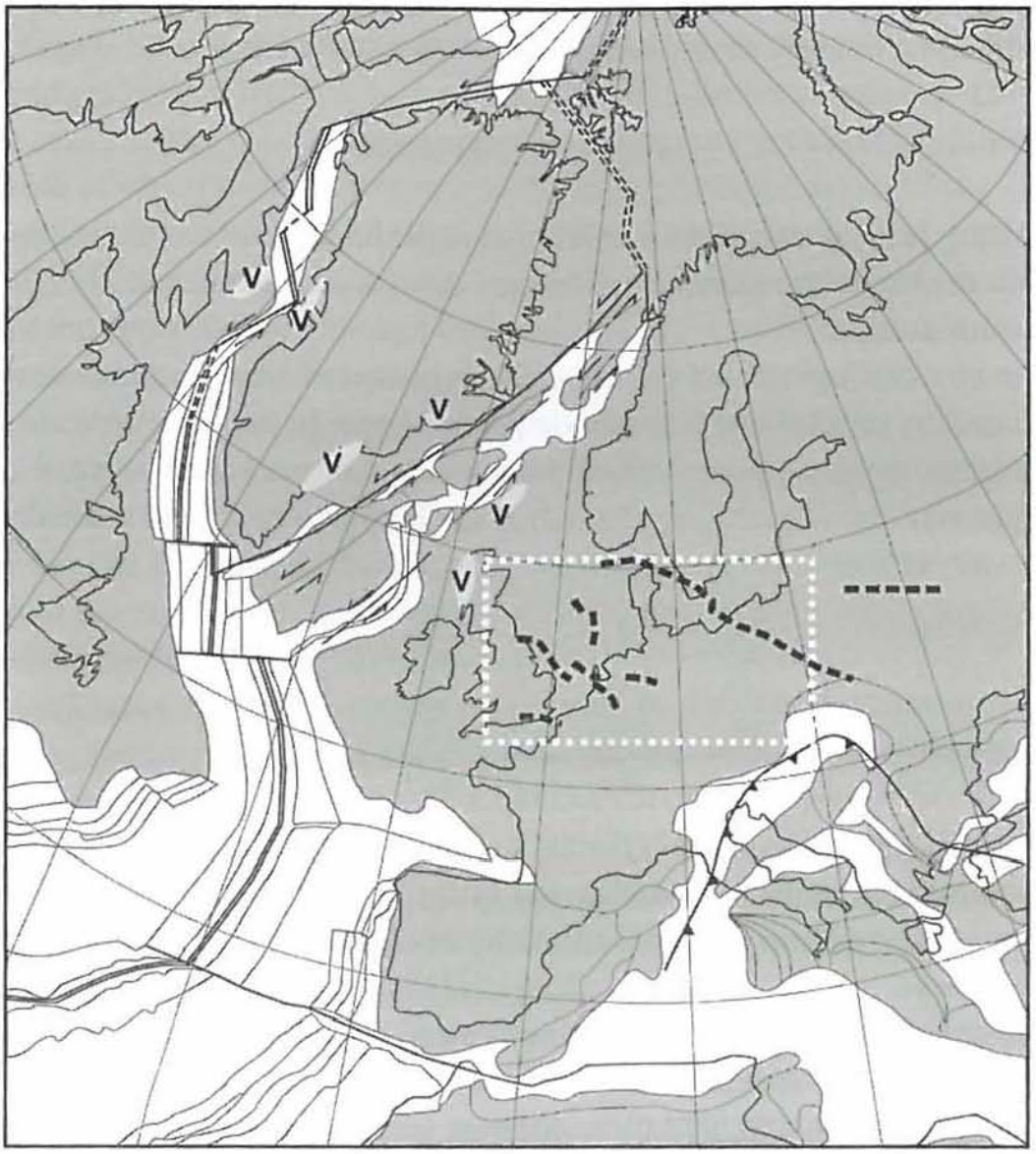


Figure 10.1 North Atlantic plate configuration around 62 Ma, simplified from Nielsen *et al.* (2007), showing the axes of European inversion structures formed in the Late Cretaceous–Paleocene (thick black dashed lines). Grey background represents continental and continental shelf areas, white background oceanic (with the double line being the Atlantic spreading centre) and deep marine areas. Light grey areas labelled "V" represent areas of major magmatism around this time, which was also the time of "secondary inversion" of the inversion structures. White dotted box shows the location of the more detailed map of Figure 10.3.

horizontal gradients of pressure variations at the base of the lithosphere. The last gives rise to dynamic topography.

### *10.2.1 Model of lithospheric stress from potential energy variations*

Lateral variations in the density structure of the lithosphere, and lateral pressure variations in the mantle below the lithosphere due to density contrasts and related convection, mean that the lithostatic pressure obtained as the weight of the rock column above a certain depth below sea level depends on location. These differences in lithostatic pressure are balanced by (mainly) horizontal stresses within the lithosphere. It can be demonstrated that

the resulting "swell push force" (Sandwell *et al.*, 1997), $F_s$, is proportional to the vertical integral of the first moment of the anomalous density, and given by

$$F_s = g \int_0^D \Delta\rho(z) z dz \tag{10.1}$$

In Eq. (10.1), $g$ is the gravitational acceleration at the Earth's surface, $\Delta\rho$ is the deviatoric lithospheric density with regard to a reference density at depth $z$, and $D$ is the depth of isostatic compensation.

Jones *et al.* (1996) presented the classical derivation of how the fundamental entities of vertical density profiles and lithospheric potential energy lead to a vertically averaged, horizontal stress balance equation where horizontal gradients of the potential energy and the basal pressure become sources of stress in the lithosphere. For the vertically averaged deviatoric stresses the set of equations reads

$$\begin{aligned} \frac{\partial \tau_{xx}}{\partial x} + \frac{\partial \tau_{yx}}{\partial y} &= \frac{1}{L}\left(\frac{\partial E}{\partial x} + L\frac{\partial \tau_{zz}}{\partial x}\right) \\ \frac{\partial \tau_{xy}}{\partial x} + \frac{\partial \tau_{yy}}{\partial y} &= \frac{1}{L}\left(\frac{\partial E}{\partial y} + L\frac{\partial \tau_{zz}}{\partial y}\right) \end{aligned} \tag{10.2}$$

In Eq. (10.2), $x$ and $y$ are local horizontal coordinates, $\tau_{xx}$, $\tau_{yy}$, and $\tau_{xy}$ are the horizontal deviatoric stresses, $E$ is the potential energy of the lithosphere of thickness $L$, and $\tau_{zz}$ is the average vertical deviatoric stress caused by deviations of the mantle pressure from a reference pressure.

A number of studies with different focuses on the major stress sources have investigated lithospheric stresses. Gosh *et al.* (2009) calculated the geopotential stress field of a mainly crustal model (based on CRUST2.0) in different isostatic states. Lithgow-Bertelloni and Guynn (2004) took a similar approach to the crustal contribution to the geopotential stresses and introduced vertical and horizontal mantle tractions. The approach of Bird *et al.* (2008) included geopotential, plate boundary, and basal stresses. They compared their results to observed seafloor spreading rates, plate velocities, anisotropy measurements, and principal stress directions. In general, the main conclusion of all these approaches was that one main driving force is not sufficient to explain the observations. A geopotential stress component is as important as basal mantle tractions and boundary forces to form the Earth's lithospheric stress field.

The present approach is similar but not identical to Jones *et al.* (1996) and differs from those of Lithgow-Bertelloni and Guynn (2004) and Bird *et al.* (2008) by considering only lithospheric potential energy and radial tractions. Plate velocities, shear tractions, and plate boundary forces are not considered.

Using CRUST2.0 (Bassin *et al.*, 2000; http://igppweb.ucsd.edu/~gabi/rem.html) we determine the potential energy of the lithosphere by isostatically balancing one-dimensional lithospheric columns in the presence of lateral pressure variations causing dynamic topography. In other words, we transfer some of the isostatic imbalance of the CRUST2.0 model to a basal pressure that supports topography. In the oceans we use the standard plate model

(Stein and Stein, 1992). The space between the reference depth (250 km) and the base of the lithosphere is filled with asthenosphere with a temperature that decreases upward along the adiabatic gradient of 0.6 °C/km at a reference potential temperature of 1315 °C (e.g., McKenzie *et al.*, 2005). This determines the temperature at the base of the lithosphere, the a-priori depth of which is obtained from a seismologically based model (Gung *et al.*, 2003; Conrad and Lithgow-Bertelloni, 2006). The CRUST2.0 model includes suggestions for the thicknesses and densities of sediment, upper crust, middle crust, and lower crust, and densities of the upper mantle although these values are not perfectly known. Furthermore, the pressure and temperature variations at the compensation depth are unknowns for which additional data in the form of topography and heat flow (Pollack and Chapman, 1977) are required to constrain the system. We consider this as an inverse problem and take the parameters of the lithospheric units as given by CRUST2.0 as tightly constrained inversion variables, the lithospheric thickness, the radiogenic heat production rate of the crust and the basal pressure as less constrained variables, and invoke a fixed coupling between basal pressure and temperature. By allowing the latter to exhibit up to ±50 °C variations around the reference potential temperature, this inverse problem is sufficiently constrained by topography and heat flow. The basal pressure variation is parameterised using a spherical harmonic polynomial of degree 16 with a total of 153 variable parameters. The resulting model satisfies topography and (largely) heat flow by means of isostatically compensated lithospheric columns of almost known structure and basal pressure (and temperature) variations. This in turn determines the global lithospheric potential energy in the presence of a basal pressure, i.e., the source terms of Eq. (10.2).

To obtain the stresses of Eq. (10.2) we use a three-dimensional, spherical, global finite element mesh of flat, thick, elastic triangles each with 15 degrees of freedom. Each triangle has three corner nodes, each with three spatial coordinates, yielding 9 degrees of freedom. Each node is furthermore bestowed with a vertical axis with 2 angular degrees of freedom, pointing initially towards the centre of the sphere, but which upon loading can deviate slightly from the vertical by pivoting around the mid plane of the element as measured by the (small) angles. This accounts for the remaining 6 degrees of freedom. The relationship between strains and stresses for this thick element is given by Zienkiewicz (1977, Chapter 16). Each element furthermore has material parameters in the form of Young's modulus, Poisson's ratio and thickness, $h$.

### *10.2.2 Predicted lithospheric stress from potential energy variations in the Europe–North Atlantic area*

The results of the global three-dimensional stress calculation (Figure 10.2a) are presented in terms of principal horizontal stress directions and magnitudes at the centre of the triangles. Effective stress, which is the square root of the second invariant of the deviatoric stress tensor, is also displayed. Our computed principal stresses compare favourably to previous models (e.g., Lithgow-Bertelloni and Guynn, 2004; Bird *et al.*, 2008) even though we

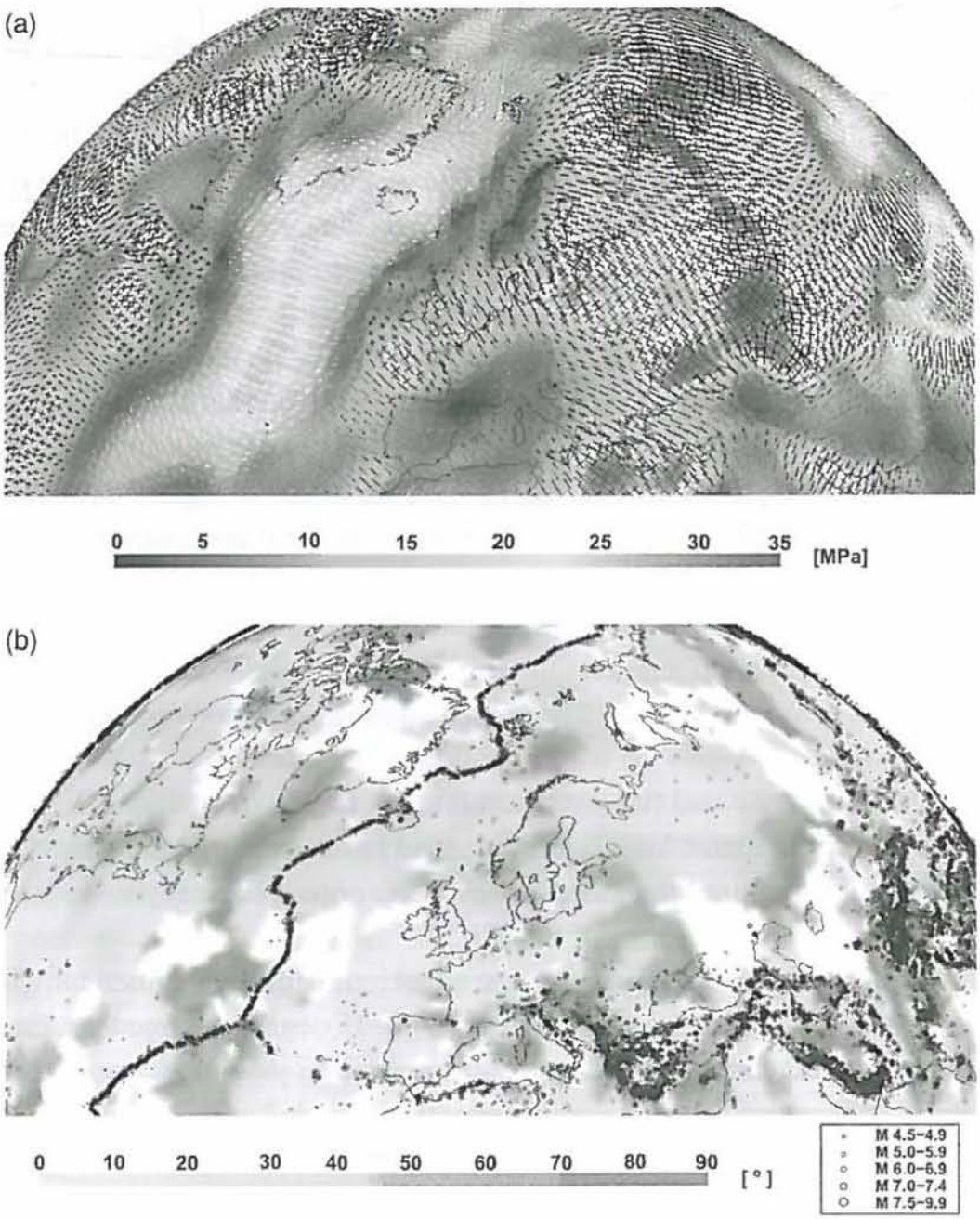


Figure 10.2 Lithospheric stress from potential energy variations. (a) Principal horizontal stress (white is extension and magenta is compression, relative to the lithostatic state of stress, where vector length represents stress magnitude) on a background of effective stress (i.e., the square root of the second invariant of the deviatoric stress tensor; e.g., Ranalli, 1995) in MPa (colour bar). (b) Difference between model predicted and observed principal stress directions (Heidbach *et al.*, 2007a, b) in degrees (colour bar: blue is a good fit and orange is a bad fit), also showing all magnitude greater than or equal to 4.5 earthquake epicentres since 1973 taken from the National Earthquake Information Centre. For colour version, see Plates section.

have not considered plate velocities, shear tractions, and plate boundary processes. The explanation could be that in the North Atlantic realm it is lithospheric potential energy and radial mantle tractions that exert the governing control on geopotential stresses. Indeed, we find that the combined stress field from radial tractions and lithospheric structure agrees better with the observed stress directions (Global Stress Map; Heidbach *et al.*, 2007) than if each source is considered individually.

The principal horizontal stresses are the vertically averaged deviatoric stresses relative to the lithostatic stress state, in which stresses (or pressure) at any depth are equal in any direction and equal to the weight of the overburden. To obtain the associated tectonic forces (N/m), the stresses should be multiplied by the thickness of the elastic shell, which is 100 km. The principal horizontal stress directions are compared to observed values (where available, from the Global Stress Map; Heidbach *et al.* [2007a, b], spatially averaged and extrapolated) and seismicity since 1973 in Figure 10.2b.

In the present context we wish to highlight the relationship between the stress field of oceans and that of the adjacent continental areas. Mature oceanic areas such as the central Atlantic Ocean clearly demonstrate the existence of ridge push in the form of relative compression of the older and deep parts of the oceanic lithosphere. Ocean ridges exhibit relative extension perpendicular to the spreading axis, but in the North Atlantic the Icelandic melt anomaly and the associated anomalous elevation of the ocean floor bear witness to a much more active spreading system. This anomaly produces a SE-directed maximum horizontal compressional stress field, which radiates from the Icelandic area through the British Isles and into central Europe, a model prediction that is in excellent agreement with observed directions of maximum compressional stress in this region (Figure 10.2b). However, it appears that the effect of the high potential energy and basal pressure in the North Atlantic around Iceland is not sufficient to place the highlands of southern Norway under significant compression. Rather, there is slight extension, which was also the conclusion of Pascal and Cloetingh (2009) using a one-dimensional approach.

We note that the conjugate Norwegian and Greenland margins exhibit very different stress states in the present model. While the Norwegian coastal areas generally are in a neutral to slightly compressive state of stress, the east Greenland coastal areas are in a state of relative extension. Apparently, this pattern correlates with the occurrence of extensive North Atlantic breakup magmatism (<62 Ma), which profoundly affected the central East Greenland oceanic and continental areas, but was far offshore on the continental shelf of western Norway. The dominant NW–SE direction of the axes of the intrusions of the British Tertiary Igneous Province (England, 1988) delivers further evidence of a correlation between the present-day potential energy related stress field and Paleocene North Atlantic magmatism. As dyke emplacement preferentially occurs within planes perpendicular to the direction of the minimum principal stress, $\sigma_3$ (Anderson, 1951), it appears that the predicted stress field of the British Isles (Figure 10.2a) with NE–SW relative extension has changed little from the stress field that furnished the overriding control on dyke emplacement in the Paleocene.

## 10.3 Past intraplate basin inversion in Europe

### *10.3.1 Style of Late Cretaceous–Paleocene basin inversion in Europe*

Common to the west-central European structures are that the zones of inversion are Late Paleozoic–Mesozoic sedimentary basins and rifts that formed during the breakup of Pangaea

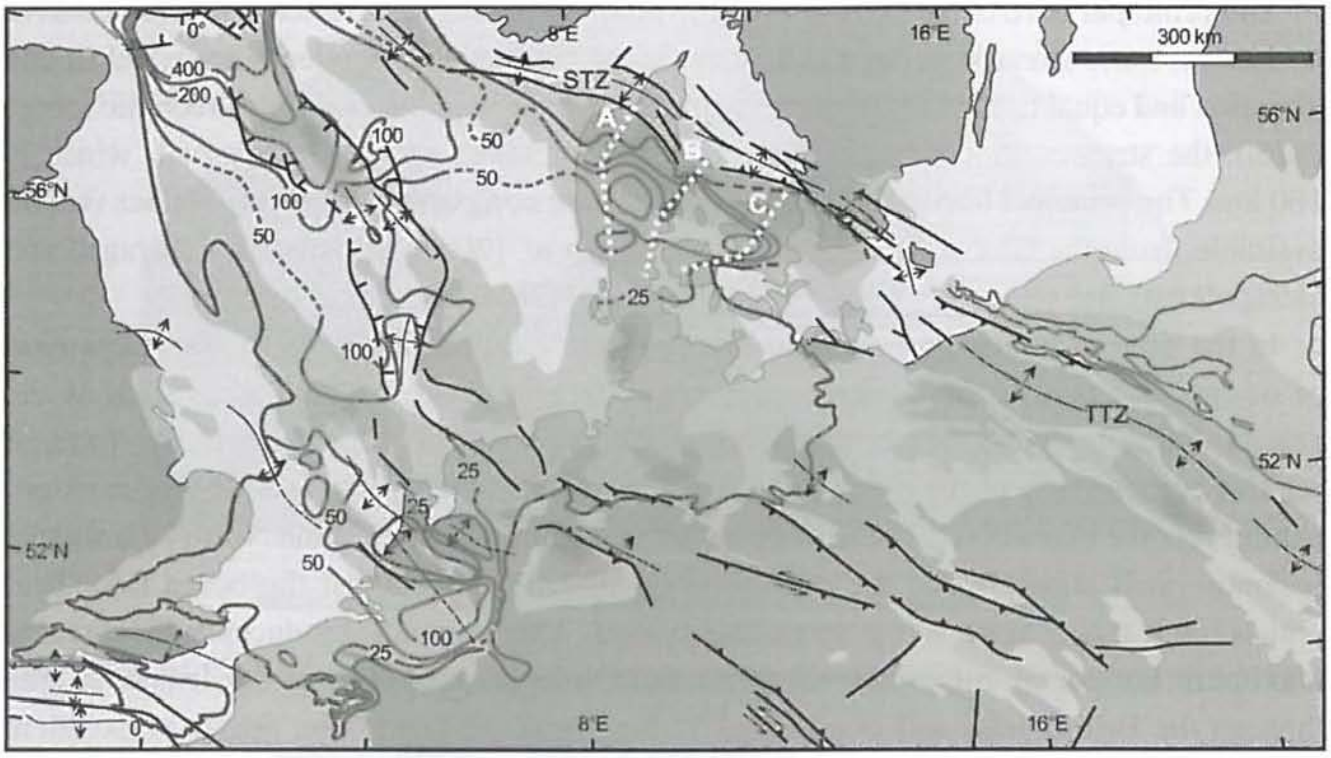


Figure 10.3 Inversion structures on the European continent (axes with anticline symbols) and the thickness of Late Cretaceous–Danian depocentres (yellow to brown colours increasing from 0–500 m, 500–1000 m, 1000–1500 m and >1500 m, respectively) and Middle–Late Paleocene depocentres (blue contours – labels in metres – with the red line indicating the depositional limit). The asymmetrical depocentres of the former are related to the primary, compressional, inversion and the more symmetrical and shallower Paleocene depocentres are related to secondary, relaxation, inversion. The depocentre east of the TTZ in Poland bounded by the green line represents Paleocene deposits <50 m. STZ is the Sorgenfrei–Tornquist Zone; TTZ is the Tornquist–Teisseyre Zone. The dotted white lines are the approximate locations of geological cross-sections (A, B, and C) shown in Figure 10.4. (The figure has been adapted from Nielsen *et al.* (2005).) For colour version, see Plates section.

(Ziegler *et al.*, 1995; Gutiérrez-Alonso *et al.*, 2008). The shallow manifestations of basin inversion are eroded ridges of up to some hundred kilometres length and of (order of magnitude) 50 km width. Flanking such zones are wider sedimentary depocentres (marginal troughs), which show a characteristic deepening towards the border faults of the uplifted zone as seen in the Upper Cretaceous–Paleocene thickness map of Europe (Figure 10.3). The internal structure of the uplifted area is characterised by reversely activated faults and thrusts, and erosion depths of up to some kilometres. It is characteristic that it is the same structures that have been reactivated over and over again.

The inversion movements occurred in phases. The earliest phase dates back to the Turonian of the early Late Cretaceous (Vejbæk and Andersen, 1987, 2002; Ziegler, 1987, 1990; Dadlez *et al.*, 1995; Ziegler *et al.*, 1995), and is believed to have heralded the change of the transtensional stress regime responsible for the breakup of Pangaea to an over-all transpressional stress regime produced by the African–European convergence and, indeed, the onset of continent–continent collision in the Alpine Orogeny (Eo-Alpine orogenic phase; e.g., Ziegler, 1990). The Late Cretaceous inversion phases were characterised by

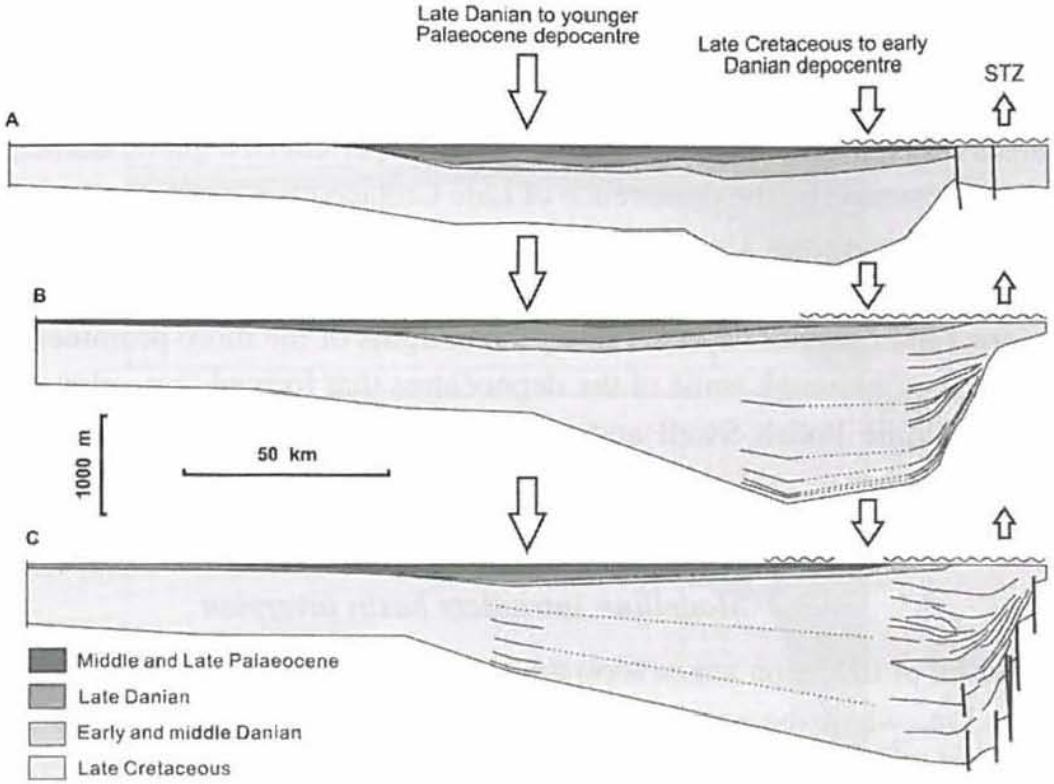


Figure 10.4 Geological profiles constructed from detailed subsurface data across the Sorgenfrei–Tornquist Zone (STZ) in Denmark and the associated sedimentary deposits (modified from Nielsen *et al.*, 2005). The northwestern part (profiles A and B) was mildly inverted and the southeastern part (profile C) was strongly inverted. Late Cretaceous deposition occurred during the primary, compressional, inversion. The shallow and symmetrical Paleocene sequence was deposited during the secondary, relaxation, inversion. For colour version, see Plates section.

transpressional shortening involving reverse activation of former normal faults and the creation of thrusts. During this phase the asymmetric marginal troughs formed (Figure 10.3). In the middle Paleocene, the European inversion structures experienced a distinct tectonic event that differed in style from the Late Cretaceous convergence-related phases. Now the inversion ridges experienced a domal, generally non-ruptural uplift, which involved both the Late Cretaceous inversion ridge and the proximal areas of the marginal troughs. Simultaneously, secondary, shallow and more symmetrical marginal troughs formed in more distal positions.

The occurrence of the two structurally distinct inversion phases is particularly well documented in the Sorgenfei–Tornquist Zone (STZ) of the Danish Basin (Figure 10.4), but their existence can also be inferred from the results of detailed studies of other structures (Vejbæk and Andersen, 2002; de Lugt *et al.*, 2003; Kockel, 2003; Lamarche *et al.*, 2003; Worum and Michon, 2005). Along the STZ the first inversion phase is visible in the asymmetrical chalk depocentre that formed mainly during the Campanian and Maastrichtian. This is evidenced by the thinning of internal chalk structures onto the inversion ridge and the embedded sandstone body that was shed into the chalk basin from source areas along the inversion ridge of southern Sweden (Erlström *et al.*, 1997). The detailed stratigraphic resolution reveals that the primary phase of inversion continued through the early and middle Danian. The onset

of the secondary inversion phase occurred during the late Danian (lasting approximately from 62 to 61 Ma) when the depocentre shifted away from the inversion ridge to a more distal position and became more symmetrical. Simultaneously, the inversion ridge and the proximal areas of the asymmetrical marginal trough experienced a gentle doming, the erosion of which is revealed by the occurrence of Late Cretaceous cocolites in early Selandian sediments (Clemmensen and Thomsen, 2005; Nielsen *et al.*, 2005; Steuerbaut, 1998). It is apparent from Figure 10.3 how the secondary phase of inversion has exerted control on the Late Paleocene (and Eocene) deposits along the margins of the more prominent European inversion structures, although some of the depocentres that formed (e.g., along the eastern margin of the Middle Polish Swell and the Weald-Boulonnais area) initially were in a non-marine setting.

### *10.3.2 Modelling intraplate basin inversion*

The typical width of inversion zones is on the order of a couple of lithosphere thicknesses, i.e., 200–250 km, when the extent of the marginal troughs is included. This order of magnitude wavelength points to a whole lithosphere involvement. The challenge is that a quantitative model of basin inversion must address both the relatively narrow localisation of shortening in the deeper parts of former sedimentary basins, the formation of marginal troughs, and the change of inversion style seen in the middle Paleocene in Europe.

The process of basin formation modifies the overall thermal and rheological structure of the lithosphere and it is obvious that this modification somehow is relevant to the later localisation of structural inversion. One fundamental question is simply why sedimentary basins are readily reactivated in compression. Although the mere existence of a sedimentary basin indicates the presence of a structural weakness in the continental lithosphere, it is not trivial how sedimentary basins can be reactivated a long time after formation, as is the case in Europe where the inversion structures generally are associated with Paleozoic and Mesozoic rift systems (Ziegler *et al.*, 1995).

The thermal and structural changes implied by extensional basin formation involve processes that both reduce and increase the load-carrying capacity of the lithosphere. For example, Braun (1992), Ziegler *et al.* (1995), van Wees and Beekman (2000), and Sandiford *et al.* (2003) pointed out that the formation of a rift basin elevates and strengthens (over time) the mantle beneath the basin because of the long-term cooling effected by the shallowing of the mantle and the attenuation of crustal heat production. This mainly thermal aspect should work against a later reactivation of the basin centre. Indeed, analysis of the subsurface temperature field in thermally equilibrated rifts has revealed (Sandiford, 1999; Sandiford *et al.*, 2003; Hansen and Nielsen, 2003) that a wide range of plausible values for the controlling parameters (thermal conductivities, heat production rates and their distribution, and the basin aspect ratio) result in a cooler upper mantle beneath the rift, while the mantle is warmer and therefore weaker beneath the margins of the rift. The fundamental mechanism here is refraction of heat around the relatively poorly conducting sediments and reduced crustal heat generation where the crust has been thinned.

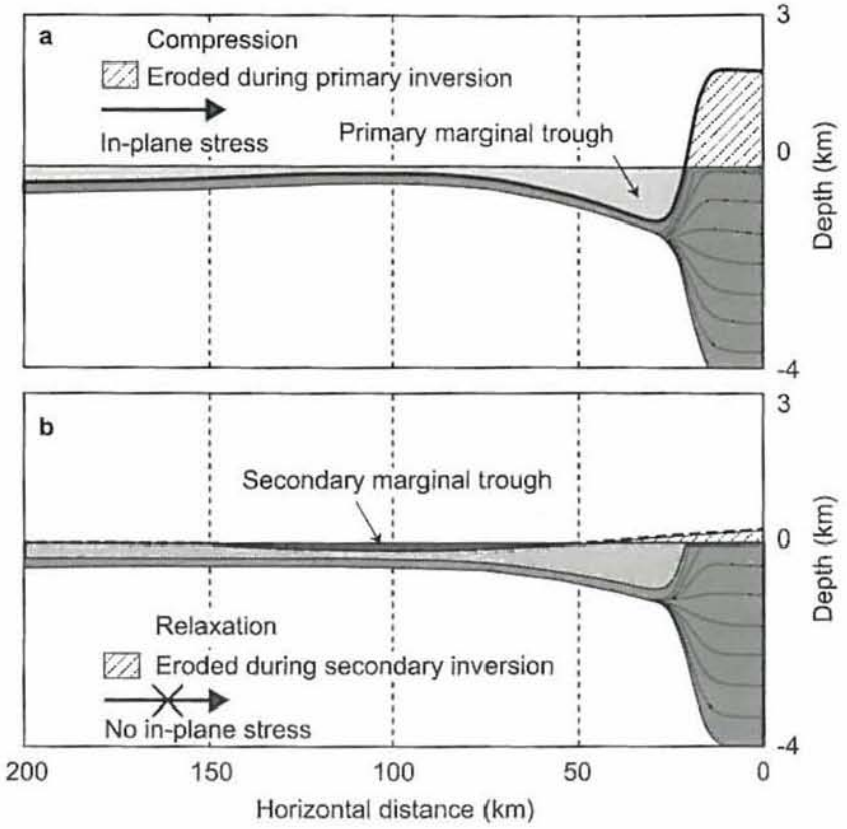


Figure 10.5 The primary and secondary inversion mechanisms: (a) basin fill after primary inversion, which occurs as a response to in-plane compression of a pre-existing rift zone; (b) basin fill after secondary inversion, which occurs as a response to relaxation of the earlier in-plane compression. Details of the modelling can be found in Nielsen *et al.* (2005).

On the other hand, the thinning of the crust during rifting, and the filling of the rift with sediments reduce the overall load-carrying capacity of the lithosphere because (1) less competent sediments have replaced more competent crustal rocks; (2) sediments are less dense than crustal rocks, reducing the confining pressure and thereby the strength of the crust below the sediments as compared to crust at the same depth outside the basin; (3) the crust beneath the sediments is likely to be warmer and therefore weaker than crust at the same depth outside the basin because of sediment blanketing; and (4) formation of crustal scale extensional faults that can be reactivated potentially have strong implications for the possibility of later inversion. Furthermore, the thermal refraction aspect of thermally equilibrated rift basins can in itself promote a strain energy favourable mode of basin inversion (Stephenson *et al.*, 2009).

Numerical modelling allows for investigating the relative importance of such oppositely directed mechanisms. Thus, assuming that a rift remains weak after its formation because of the wealth of faults that are produced during rifting, Nielsen and Hansen (2000) constructed a numerical thermo-mechanical model of compressional basin inversion that reproduced the fundamental observational features of inversion structures on the European continent (Figure 10.5). The model response to compression was localised shortening, thickening, and uplift of the upper crust and sediments within the rift, while the lower crust and upper mantle became slightly depressed. Simultaneously, syn-compressional and asymmetric marginal

troughs formed on the former rift flanks. The model suggested that the shortening of crust and sediments is accommodated by shortening also in the lithospheric mantle in the vicinity of the rift, where the upper mantle is slightly warmer and therefore weaker. The occurrence of the asymmetrical marginal troughs was explained in this model by flexural loading of the lithosphere by the internal lithospheric load (as compared to the pre-inversion situation) that formed along the inversion axis because of thickening of the crust in the inversion zone and the replacement of less consolidated near-surface sediments with deeper and denser sediments. The most compelling proof for the existence of this lithospheric load along the inversion axis is the longevity of the asymmetric sedimentary depocentres flanking the European inversion structures (e.g., Figure 10.3). In some cases the axial load is also visible in a slightly elevated Bouguer gravity anomaly along the inversion trend (Wybraniec *et al.*, 1998).

Nielsen and Hansen's (2000) model also predicts the occurrence of "secondary inversion" (Figure 10.5). The mechanism here is that the compression during the primary inversion phase over-deepens the lithospheric flexure that is produced by the axial load of the inversion structure. During the convergence phase the lithosphere is relatively stiffer because the ongoing straining works against the continuous viscous relaxation of the stresses that are generated. When compressional stresses cease or decrease, the lithosphere performs a vertical, elastic flexural adjustment to the new boundary condition (not dissimilar to the mechanism described in Braun and Beaumont [1989]) in the form of an upward doming (order of magnitude $10^2$ m) of the central inversion zone and the proximal areas of the primary marginal troughs, and a flexural down warp of smaller amplitude at a greater distance. The undulation continues beyond the elastic flexural adjustment, driven by viscous relaxation of stresses in the softer parts of the lithosphere and the associated regional isostatic adjustment.

## 10.4 Discussion

The computed stresses described in Section 10.2 and illustrated in Figure 10.2 are those derived from models of lateral variations in the present-day density structure of the lithosphere and lateral pressure variations in the mantle below the lithosphere due to density contrasts and related convection (i.e., variations of potential energy of the lithosphere and basal pressure). We will refer to these stresses as the "potential energy" stresses in the ensuing discussion. Figure 10.2b shows that these, expressed in terms of principal stress orientation, are largely incompatible with observed principal stresses, where available (e.g., Heidbach *et al.*, 2007a, b), in zones where the bulk of present-day seismicity occurs, which is along or close to active plate boundaries, as exemplified by the Tethyan convergence zone from the Mediterranean through central Asia.

This incompatibility demonstrates quite succinctly that interplate deformation (as expressed here as seismicity near a plate boundary) is driven by stresses heavily dominated by forces developed by plate interactions at plate boundaries. However, away from active plate boundary zones, Figure 10.2b shows that there is generally a good fit between

predicted and observed stress directions where observed stress data are available. There is even the possibility of a vague correlation between intraplate seismicity (cf. central Europe) and regions where this good fit is seen, although we have made no attempt to determine any quantitative significance of this. In any case, it is fair to infer that intraplate stresses in Europe (that is, away from zones of convergence) are those being generated by potential energy effects rather than plate boundary effects. And, although there is some seismicity in such regions, there is no evidence, nor do our results suggest, that geologically significant intraplate deformation (i.e., basin inversion) is occurring at this time.

These correlations (good fit between modelled and observed stresses at the present day in intraplate settings and bad fit in tectonic plate boundary settings) in the context of the geological record of Late Cretaceous–Paleocene basin intraplate inversion in Europe allow us to make some inferences about cause and effect in intraplate deformation.

First, the potential energy stress field (Figure 10.2) is not in itself sufficient (for typical continental lithosphere composition, heterogeneity, and thermal structure) to produce geologically significant deformation, as recorded by what Nielsen and Hansen (2000) called "primary inversion" of basins in Europe (Figures 10.3–10.5). Rather, the main source of intraplate stress in driving intraplate strain expressed as such is that derived at plate boundaries. These stresses are of course superimposed upon the stresses derived from potential energy variations within the lithosphere. However, primary inversion occurs only when very high plate boundary forces combine favourably with potential energy "background" intraplate stresses (e.g., Figure 10.2a) in combination with the existence of pre-existing lithosphere-scale weaknesses that are also favourably orientated. The crustal geometries that are behind this are to some extent themselves a consequence of the processes that led to basin formation in the region in the first place. Nevertheless, intraplate primary basin inversion in Europe results not only from stresses building up – mainly from forces developed at a plate boundary convergent setting – but also depends on finding favourable rift-like structures amenable to reactivation as well as a favourable interaction (interference) of those stresses with the intrinsic "background" potential energy stress field.

Second, there is clear evidence to link the dissipation (relaxation) of the extraordinary stress field that caused primary inversion, derived mainly from plate boundary forces, to the occurrence of what Nielsen and Hansen (2000) called "secondary" basin inversion. This indirectly supports the inference that it was indeed the plate boundary derived stresses causing the primary inversion in the first place. Nielsen *et al.* (2007), following discussion by Nielsen *et al.* (2005), demonstrated that the relaxation of plate convergence derived stresses was the key factor explaining very precisely dated shifts in deposition patterns within the Danish Basin in the middle Paleocene (62 Ma). Possible causes for such a sudden plate-wide stress change suggested by Nielsen *et al.* (2005) were the Paleocene slowing down of the African–European convergence (e.g., Rosenbaum *et al.*, 2002) or the creation of a new plate margin in the North Atlantic (e.g., Harrison *et al.*, 1999) at the time of arrival of the proto Icelandic plume at the base of the North Atlantic lithosphere during the late Danian, slightly prior to the Danian–Selandian boundary (~62 Ma). However, the potential energy derived lithosphere stresses thought to be developed at this time with the postulated arrival

of the Iceland plume and the initiation of the NAA, are actually directly incompatible with the observed secondary inversion deposition patterns (Nielsen *et al.*, 2007). These authors went on to point out that their stress modelling argued against a plume model for the tectonic evolution of the North Atlantic in the Paleocene. Rather, they proposed that magmatism and other North Atlantic tectonic events around this time were the consequence of changes to plate boundary interactions, specifically an embryonic strike-slip initiation of the North Atlantic plate boundary between Greenland and Scandinavia.

Third, we might presume that structures formed during pre-inversion rifting must also play a role in primary basin inversion, specifically that they should be favourably orientated with respect to the build-up of the causative tectonic convergence stress field. The importance of compressional reactivation of faults formed during extensional basin formation was noted by Buiter and Pfiffner (2003) and investigated in more detail in numerical experiments by Hansen and Nielsen (2003). By adjusting the degree of strain softening in three models they found that faults produced during rifting that remain weak, and thereby easily reversible, have the potential to influence profoundly the load-carrying capacity of the lithosphere and hence the future deformation history. The overall structural elements of the inverted rifts (a central inversion ridge flanked by asymmetrical marginal troughs) remained robust features of their models, similar therefore to the model of Nielsen and Hansen (2000). Regarding the orientation of reactivated structures in central Europe, it may simply be an intraplate setting fortuitous for basin inversion, with basement trends basically formed during late Paleozoic orogenesis (e.g., Ziegler *et al.*, 2006) being amenable to the particular plate boundary force derived stresses related to later collision with Africa.

An interesting result of the stress model presented here is that the potential energy stresses, expressed as effective stress (Figure 10.2a), are very small in the region of Europe that tends to have been most affected by intraplate basin inversion. This is the zone running from the North Sea and Denmark southeastwards to the Black Sea, corresponding to the "Trans-European Suture Zone" (TESZ; e.g., Pharaoh *et al.*, 2006) between cratonic lithosphere to the east and mostly younger accreted terranes to the west. The present-day stress field in this area is not one dominantly reflecting the NAA (which in any case was not yet in existence at the time of basin inversion) but has more to do with intrinsic lithosphere structure in the TESZ (which was already in place at that time). Though pre-existing structure and thermal refraction effects must have played a role, it is possible that the absence of a potentially counteracting "background" potential energy stress field in this area (i.e., similar to what is computed for the present day) may have been a factor in allowing the plate boundary derived stress field to be highly effective in causing intraplate deformation in this part of Europe.

## 10.5 Summary and conclusions

According to plate tectonics, lithospheric plates are essentially rigid with deformation resulting from interactions along (or very near) plate boundaries. In this respect basin inversion is an intermediate-scale manifestation of continental intraplate deformation,

which, together with the occurrence of aseismic creep, distributed earthquake activity and the large-scale, large-amplitude deformations such as the Indian–Asian collision, testifies to the well-established deviation of large areas of the interior of continents from rigid plate tectonics. The inverted sedimentary basins of central Europe represent a classic example of this phenomenon. We have reviewed the dynamics of how inversion has occurred in these basins, where tightly constrained observations of the timing of vertical motions reveals that it occurs in two phases. The first phase, which in Europe begins in the early Late Cretaceous, displays transpressional shortening involving reverse activation of former normal faults and the creation of thrusts driven by stresses primarily derived from forces developed at the convergent southern margin of the Europe plate. The second phase, which in Europe occurs in the middle Paleocene, displays generally non-ruptural uplift of the earlier developed inversion ridge and the formation of shallow marginal troughs in more distal positions and is related to the lithosphere's response to the relaxation of the stress field responsible for the first inversion phase. The cause and effect relationship of intraplate stresses and intraplate deformation in Europe in the Late Cretaceous and Paleocene has been indirectly illuminated by considering a model of that part of the present-day stress field of Europe (and the North Atlantic) caused by potential energy variations in the present-day lithosphere. An important feature of intraplate basin inversion in Europe is that the causative stress field must have been favourably orientated with respect to pre-existing structures in the lithosphere and, further, that the stresses derived from plate boundary forces have not been destructively interfered with by the stresses derived from potential energy variations.

## References

Anderson, E. M. (1951). *The Dynamics of Faulting and Dyke Formation, with Applications to Britain*. Edinburgh: Oliver and Boyd.

Bassin, C., Laske, G., and Masters, G. (2000). The current limits of resolution for surface wave tomography in North America. *Eos, Transactions, American Geophysical Union*, 81, F897.

Bird, P., Liu, Z., and Rucker, W. K. (2008). Stresses that drive the plates from below: definitions, computational path, model optimization, and error analysis. *Journal of Geophysical Research*, 113, 1406.

Braun, J. (1992). Post-extensional mantle healing and episodic extension in the Canning Basin. *Geophysical Research*, 97, 8927–8936.

Braun, J., and Beaumont, C. (1989). A physical explanation of the relationship between flank uplifts and the breakup unconformity at rifted continental margins. *Geology*, 17, 760–764.

Buiter, S. J. H., and Pfiffner, O. A. (2003). Numerical models of the inversion of half-graben basins. *Tectonics*, 22, 1057, doi:10.1029/2002TC001417.

Clemmensen, A., and Thomsen, E. (2005). Palaeoenvironmental changes across the Danian-Selandian boundary in the North Sea Basin. *Palaeogeography, Palaeoclimatology, Palaeoecology*, 219, 351–394.

Conrad, C. P., and Lithgow-Bertelloni, C. (2006). Influence of continental roots and asthenosphere on platemantle coupling. *Geophysical Research Letters*, 33, L05312, doi:10.1029/2005GL025621.

Dadlez, R., Narkiewicz, M., Stephenson, R. A., Visser, M. T. M., and Van Wees, J.-D. (1995). Tectonic evolution of the Mid-Polish Trough: modelling implications and significance for central European Geology. *Tectonophysics*, 252, 179–195.

de Lugt, I. R., van Wees, J. D., and Wong, Th. E. (2003). The tectonic evolution of the southern Dutch North Sea during the Paleogene: basin inversion in distinct pulses. In *Dynamics of Sedimentary Basin Inversion: Observations and Modelling*, ed. S. B. Nielsen and U. Bayer. *Tectonophysics*, 373, 141–159.

England, R. W. (1988). The Early Tertiary stress regime in NW Britain: evidence from the patterns of volcanic activity. In *Early Tertiary Volcanism and the Opening of the NE Atlantic*, ed. A. C. Morton and L. M. Parson, Geological Society, London, Special Publication 39, pp. 381–389.

Erlström, M., Thomas, S. A., Deeks, N., and Sivhed, U. (1997). Structure and tectonic evolution of the Tornquist Zone and adjacent sedimentary basins in Scania and the southern Baltic Sea area. *Tectonophysics*, 271, 191–225.

Ghosh, A., Holt, W. E., and Flesch, L. M. (2009). Contribution of gravitational potential energy differences to the global stress field. *Geophysical Journal International*, 179, 787–812.

Gung, Y., Panning, M., and Romanowicz, B. (2003). Global anisotropy and the thickness of continents. *Nature*, 422, 707–711, doi:10.1038/nature01559.

Gutiérrez-Alonso, G., Fernández-Suárez, J., Weil, A. B., *et al.* (2008). Self-subduction of the Pangaean global plate. *Nature Geosciences*, 1, 549–553.

Hansen, D. L., and Nielsen, S. B. (2003). Why rifts invert in compression. *Tectonophysics*, 373, 5–24.

Harrison, J. C., Sweet, A. R., McIntyre, D. J., *et al.* (1999). Correlation of Cenozoic sequences of the Canadian Arctic region and Greenland: implications for the tectonic history of northern North America. *Bulletin of Canadian Petroleum Geology*, 47, 223–254.

Heidbach, O., Fuchs, K., Muller, B., *et al.* (2007a). The World Stress Map. *Episodes*, 30, 197–201.

Heidbach, O., Reinecker, J., Tingay, M., *et al.* (2007b). Plate boundary forces are not enough: second- and third-order stress patterns highlighted in the World Stress Map database. *Tectonics*, 26, TC6014, doi:10.1029/2007TC002133.

Jones, C. H., Unruh, J. R., and Sonder, L. J. (1996). The role of gravitational potential energy in active deformation in the southwestern United States. *Nature*, 381, 37–41.

Kockel, F. (2003). Inversion structures in Central Europe: expressions and reasons, an open discussion. *Netherlands Journal of Geosciences*, 82, 367–382.

Lamarche, J., Scheck, M., and Lewerenz, B. (2003). Heterogeneous inversion of the Mid-Polish Trough related to crustal architecture, sedimentary patterns and structural inheritance. *Tectonophysics*, 373, 141–159.

McKenzie, D., Jackson, J., and Priestley, K. (2005). Thermal structure of oceanic and continental lithosphere. *Earth and Planetary Science Letters*, 233, 337–349.

Lithgow-Bertelloni, C., and Guynn, J. H. (2004). Origin of the lithospheric stress field. *Journal of Geophysical Research*, 109, B01408, doi:10.1029/2003JB002467.

Nielsen, S. B., and Hansen, D. L. (2000). Physical explanation of the formation and evolution of inversion zones and marginal troughs. *Geology*, 28, 875–878.

Nielsen, S. B., Thomsen, E., Hansen, D. L., and Clausen, O. R. (2005). Plate-wide stress relaxation explains European Palaeocene basin inversions. *Nature*, 435, 195–198.

Nielsen, S. B., Stephenson, R. A., and Thomsen, E. (2007). Dynamics of Mid-Palaeocene North Atlantic rifting linked with European intra-plate deformations. *Nature*, 450, 1071–1074.

Pascal, C., and Cloetingh, S. (2009). Gravitational potential stresses and stress field of passive continental margins: insights from the south-Norway shelf. *Earth and Planetary Science Letters*, 277, 464–473.

Pharaoh, T. C., Winchester, J. A., Verniers, J., Lassen, A., and Seghedi, A. (2006). The Western accretionary margin of the East European Craton: an overview. In *European Lithosphere Dynamics*, ed. D. G. Gee and R. A. Stephenson. Geological Society, London, Memoirs, 32, pp. 291–311.

Pollack, H. N., and Chapman, D. S. (1977). On the regional variation of heat flow, geotherms, and lithospheric thickness. *Tectonophysics*, 38, 279–296.

Ranalli, G. (1995). *Rheology of the Earth*. London, New York: Chapman and Hall.

Rosenbaum, G., Lister, G. S., and Duboz, C. (2002). Relative motions of Africa, Iberia and Europe during Alpine orogeny. *Tectonophysics*, 359, 117–129.

Sandiford, M. (1999). Mechanics of basin inversion. *Tectonophysics*, 305, 109–120.

Sandiford, M., Frederiksen, S., and Braun, J. (2003). The long-term thermal consequences of rifting: implications for basin reactivation. *Basin Research*, 15, 23–43.

Sandwell, D. T., Johnson, C. L., Bilotti, F., and Suppe, J. (1997). Driving forces for limited tectonics on Venus. *Icarus*, 129, 232–244.

Stein, C. A., and Stein, S. (1992). A model for the global variation in oceanic depth and heat flow with lithospheric age. *Nature*, 359, 123–129.

Stephenson, R., Egholm, D. L., Nielsen, S. B., and Stovba, S. M. (2009). Thermal refraction facilitates 'cold' intra-plate deformation: the Donbas foldbelt (Ukraine). *Nature Geosciences*, 2, 290–293.

Steurbaut, E. (1998). High-resolution holostratigraphy of Middle Paleocene to Early Eocene strata in Belgium and adjacent areas. *Palaeontographica A*, 247, 91–156.

Tegner, C., Duncan, R. A., Bernstein S., *et al.* (1998). 40Ar-39Ar geochronology of Tertiary mafic intrusions along the East Greenland rifted margin: relation to flood basalts and the Iceland hotspot track. *Earth and Planetary Science Letters*, 156, 75–88.

Turner, J. P., and Williams, G. A. (2004). Sedimentary basin inversion and intra-plate shortening. *Earth-Science Reviews*, 65, 277–304.

van Wees, J. D., and Beekman, F. (2000). Lithosphere rheology during intraplate basin extension and inversion: inferences from automated modelling of four basins in western Europe. *Tectonophysics*, 320, 219–242.

Vejbæk, O. V., and Andersen, C. (1987). Cretaceous Early Tertiary inversion tectonism in the Danish Central Trough. *Tectonophysics*, 137, 221–238.

Vejbæk, O. V., and Andersen, C. (2002). Post mid-Cretaceous inversion tectonics in the Danish Central Graben. *Bulletin of the Geological Society of Denmark*, 49, 129–144.

Voigt, E. (1962). Über Randtröge vor Schollenrändern und ihre Bedeutung im Gebiet der Mitteleuropäischen Senke und angrenzender Gebiete. *Zeitschrift der Deutschen Geologischen Gesellschaft*, 114, 378–418.

Worum, G., and Michon, L. (2005). Implications of continuous structural inversion in the West Netherlands Basin for understanding controls on Palaeogene deformation in NW Europe. *Journal of the Geological Society, London*, 162, 73–85.

Wybraniec, S., Zhou, S., Thybo, H., *et al.* (1998). New map compiled of Europe's gravity field. *Eos, Transactions, American Geophysical Union*, 79, 437–442.

Ziegler, P. A. (1987). Late Cretaceous and Cenozoic intra-plate compressional deformations in the Alpine foreland: a geodynamic model. *Tectonophysics*, 137, 389–420.

Ziegler, P. A. (1990). *Geological Atlas of Western and Central Europe*. Bath, UK: Geological Society of London Publishing House.

Ziegler, P. A., Cloetingh, S., and van Wees, J.-D. (1995). Dynamics of intraplate compressional deformation: the Alpine foreland and other examples. *Tectonophysics*, 252, 7–59.

Ziegler, P. A., Schumacher, M. E., Dèzes, P., van Wees, J.-D., and Cloetingh, S. (2006). Post-Variscan evolution of the lithosphere in the area of the European Cenozoic Rift System. In *European Lithosphere Dynamics*, ed. D. G. Gee and R. A. Stephenson. Geological Society, London, Memoirs, 32, pp. 97–112.

Zienkiewicz, O. C. (1977). *The Finite Element Method*, third edition. Maidenhead, UK: McGraw-Hill.

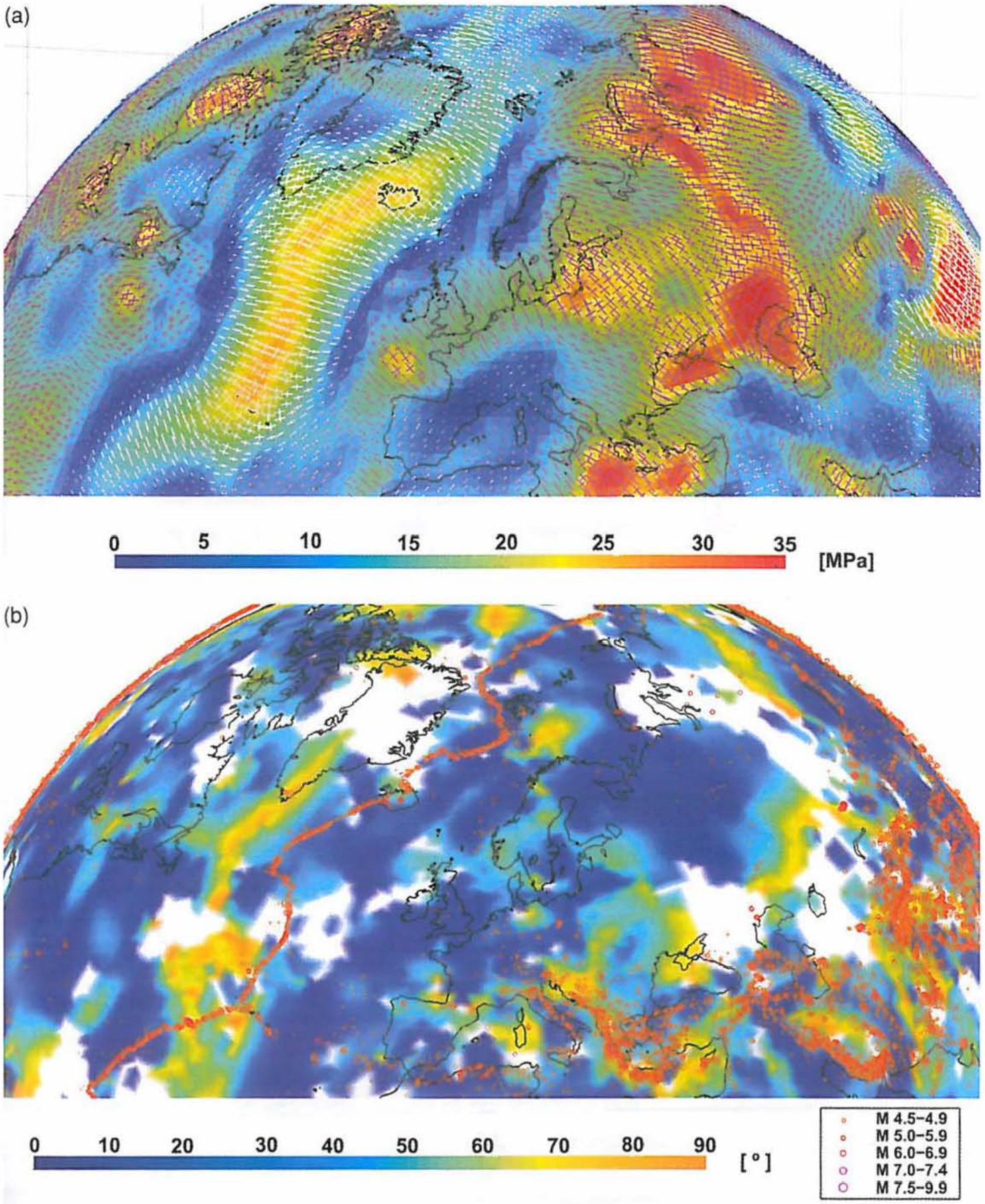


Figure 10.2 For caption, see text, p. 262.

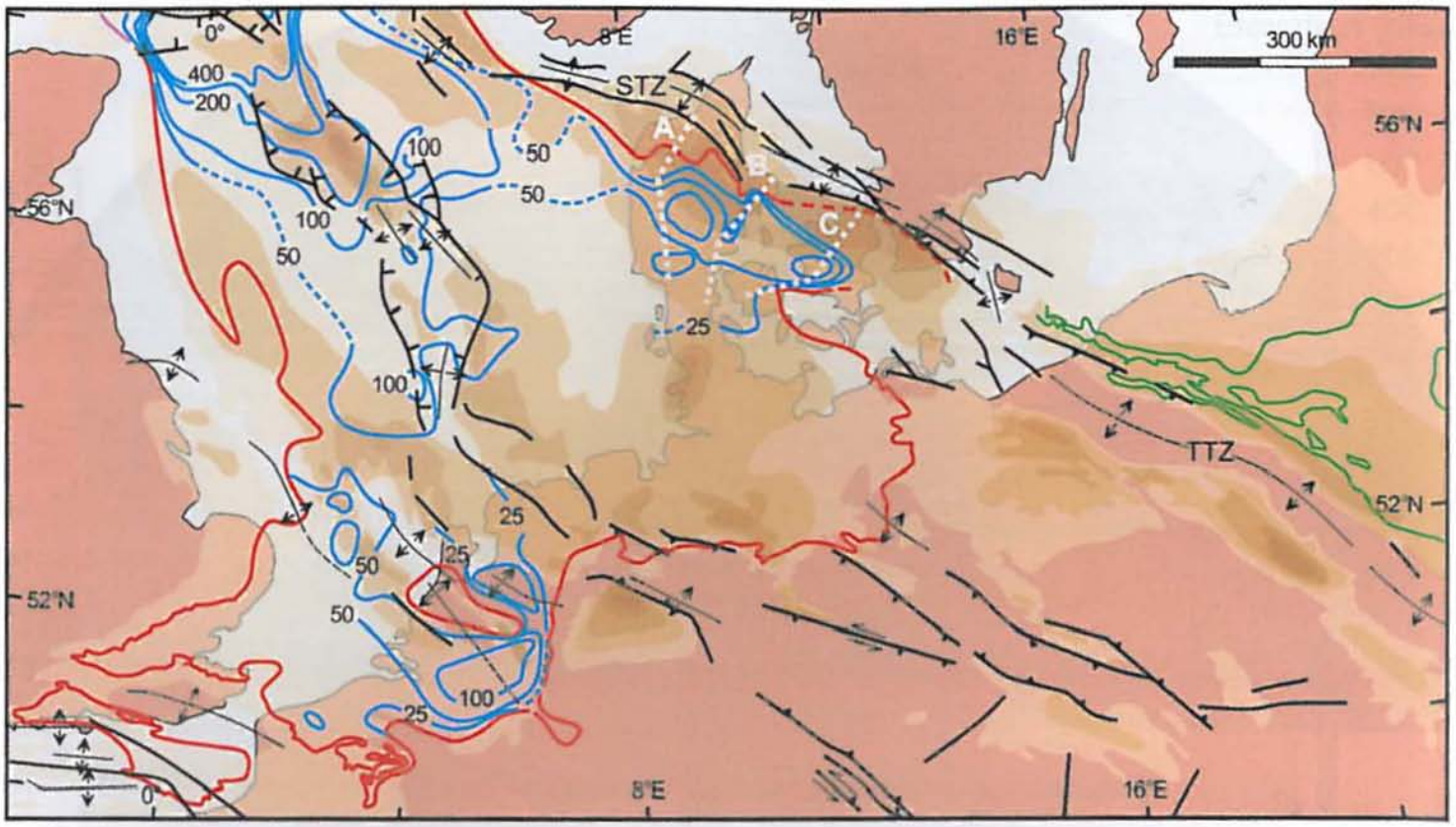


Figure 10.3 For caption, see text, p. 264.

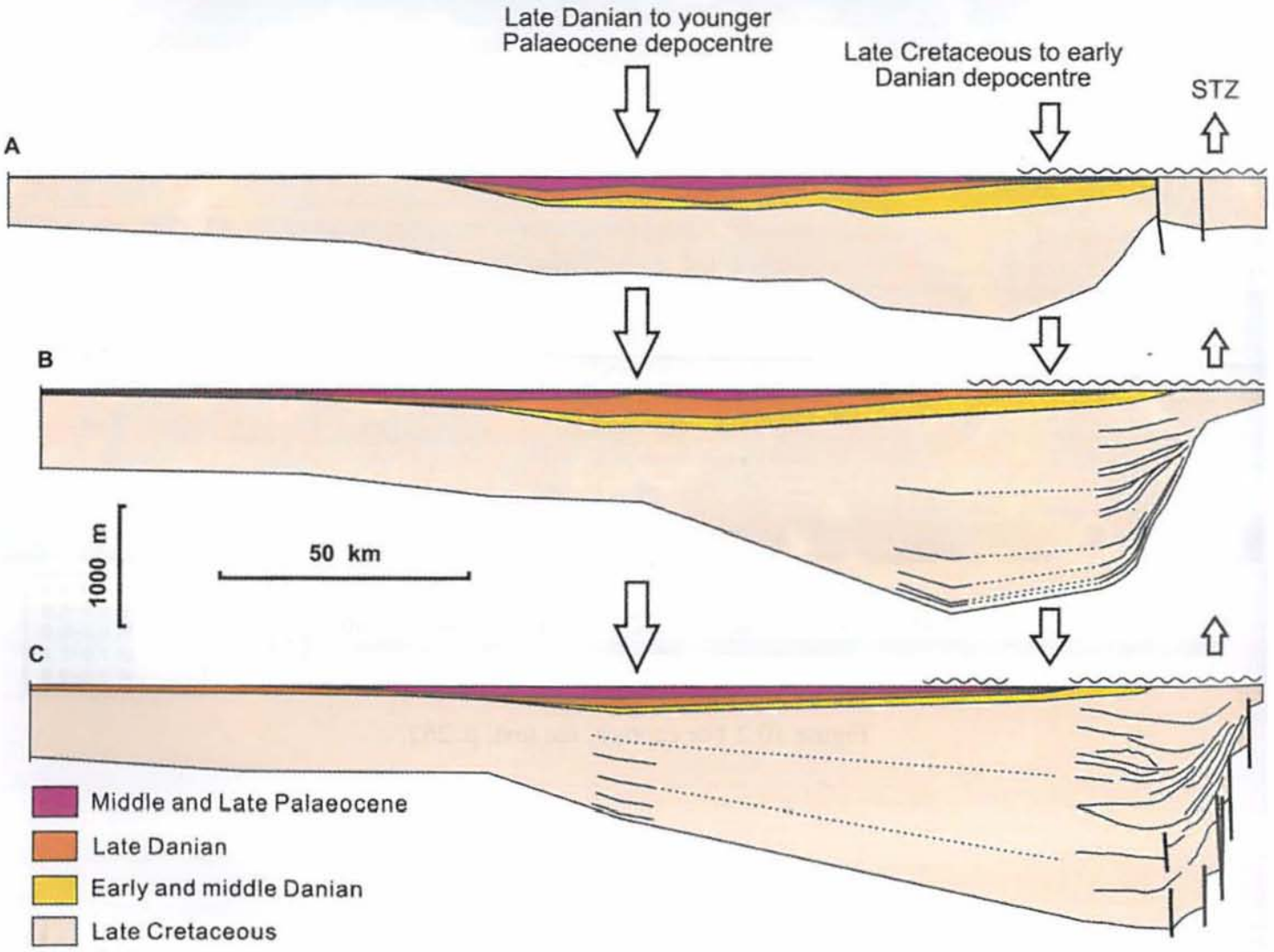


Figure 10.4 For caption, see text, p. 265.